Proceedings of the 52nd European Microwave Conference

Effective TE-Polarized Bessel-Beam Excitation for Wireless Power Transfer Near-Field Links

Edoardo Negri#1, Francesca Benassi§2, Walter Fuscaldo*3, Diego Masotti §4,
Paolo Burghignoli#5, Alessandra Costanzo§6, Alessandro Galli#7
#Dipartimento di Ingegneria dell'Informazione, Elettronica e Telecomunicazioni, Sapienza Università di Roma, Rome, Italy
§DEI "Guglielmo Marconi", University of Bologna, Bologna, Italy
*Istituto per la Microelettronica e Microsistemi, Consiglio Nazionale delle Ricerche, Rome, Italy
{1edoardo.negri, 5paolo.burghignoli, 7alessandro.galli}@uniroma1.it, 3walter.fuscaldo@cnr.it
{2francesca.benassi9,4diego.masotti,6alessandra.costanzo}@unibo.it

Abstract — **The possibility to establish a wireless link in the radiative near field at millimeter waves through Transverse Electric (TE) polarized Bessel beams is here investigated. Previous realizations of TE-polarized Bessel beams at millimeter waves are based on leaky-wave resonant cavities fed with *loop antennas*. Unfortunately, these feeders also excite undesired, nonnegligible Transverse Magnetic (TM) field components, thus leading to a *hybrid* TE polarization, rather than a *pure* TE polarization. In this work, we propose a *radial-slot array feeding* technique as an effective solution to generate almost pure TE-polarized Bessel beams in leaky-wave resonant cavities. The design is based on an effective leaky-wave approach for the characterization of the launcher. The proposed TE feeding scheme is validated with full-wave results. The study of a complete wireless power transfer scenario shows that the proposed solution significantly improves the link budget compared to previous hybrid TE- and TM-polarization cases.**

Keywords — **Bessel beams, leaky waves, resonant cavities, near-field focusing, wireless power transfer**

I. INTRODUCTION

Bessel beams (BBs) are solutions to the scalar Helmholtz equation with a remarkably focused and limited-diffraction character [1]. These features have attracted much interest in optics during the '80s [2], and more recently at millimeter waves [3]. In this latter context, it has been shown that the transverse localization of BBs along with their limited-diffraction character is beneficial in wireless power transfer (WPT) applications [4]–[6].

A device capable of producing BBs is commonly referred to as a BB launcher. In the last ten years, different BB launchers have been realized at millimeter waves (see, e.g., [3]). Among them, those based on leaky-wave resonant cavities (see, e.g., [7]–[10]) provide for a low-cost, planar, and compact solution (see Fig. 1 as a reference example). Remarkably, leaky-wave resonant cavities have a transverse size of only few wavelengths, thus being particularly attractive for realizing wearable devices for millimeter-wave WPT applications.

However, most of experiments on BB launchers deal with the Transverse Magnetic (TM) polarized case only. As a matter of fact, at microwave and millimeter-wave frequencies, coaxial feeders represent a very practical and low-cost choice. Since a coaxial feed is equivalent to a vertical electric dipole (VED), the resulting BB is inherently TM-polarized. Conversely, a Transverse Electric (TE) polarized BB would be excited by a vertical magnetic dipole (VMD), which is more difficult to realize in practice. Nonetheless, loop antennas and feeding coils have been proposed in [6], [9], [10] to excite a *quasi* TE-polarized BB. Unfortunately, these feeders also excite nonnegligible TM field components, thus a *pure* TE-polarized BB is never excited, but rather a *hybrid* polarization with a prevalent TE character [6]. It is worthwhile to stress that the generation of TE-polarized focused beams (as Bessel beams) is not only interesting from a theoretical viewpoint, but it is also of utmost importance in wearable WPT applications for mitigating dielectric losses. Indeed, as discussed in [9], the prevalent magnetic character of TE-polarized fields allow for minimizing the coupling with the surrounding lossy dielectric objects, such as human tissues.

In this context, we propose here an original feeding mechanism for leaky-wave resonant cavities capable of generating an almost *pure* TE-polarized BB. The feeding mechanism consists of a radial-slot array etched on the ground plane (see Fig. 2). Full-wave results show that the near-field distributions of the electromagnetic fields agree well with those expected from theory. The proposed launchers are then used to create a WPT near-field link. The WPT performance is evaluated in terms of link budget and compared with previous results obtained with TM-polarized and hybrid-TE BBs [6]. Results demonstrate a superior performance of the proposed radial-slot feeding scheme with respect to previous solutions.

The paper is organized as follows. Section II shows the design and full-wave validation of a TE-polarized BB launcher, whereas Section III deals with the link budget analysis of the launchers in a WPT scenario. Conclusions are finally drawn in Section IV.

II. DESIGN OF A TE-POLARIZED LEAKY-WAVE RESONANT CAVITY

A leaky-wave resonant cavity consists typically of a circular grounded dielectric slab with a partially reflecting sheet (PRS) on top and a dipole-like source in the center, as shown in Fig. 1. This architecture is common to either the TE- or the TM-polarized case. A purely TM(TE)-polarized BB is obtained by exciting the cavity in the center with

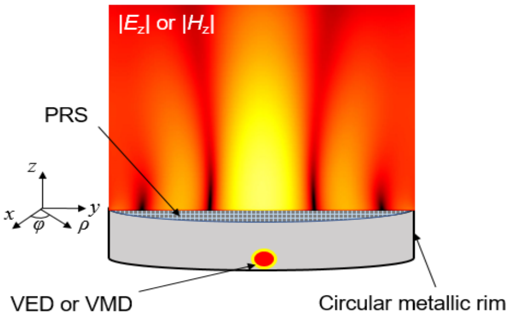

Fig. 1. Pictorial representation of a leaky-wave resonant cavity along with the theoretical near-field distribution of the E_z or the H_z field components, whether an ideal VED (TM polarization) or VMD (TE polarization) source is used to excite the cavity.

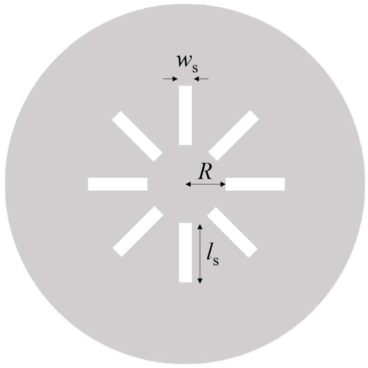

Fig. 2. A sketch of the feeding structure of a TE-polarized BB launcher: a radial-slot array with its relevant geometrical parameters.

a VED(VMD)-like source. In the TM(TE)-polarization case, the device excites a zeroth order BB over the vertical electric(magnetic) field component, as depicted in Fig. 1.

Thanks to their propagation-invariant character, BBs exhibit the same transverse profile up to a finite distance from the aperture plane. This distance z_{ndr}, also known as *nondiffractive range*, is not really affected by the polarization of the field, but depends on certain design parameters, through the following approximate ray-optics formula [2]

$$z_{\mathrm{ndr}} = \rho_{\mathrm{ap}} \cot \theta_0 \qquad (1)$$

where ρ_{ap} is the aperture radius, and θ_0 is the *axicon angle* (measured with respect to the vertical z-axis). The aperture radius is evidently determined by the geometry of the device, whereas the axicon angle is related to the peculiar radiating properties of the structure. Specifically, in leaky-wave resonant cavities the axicon angle θ_0 is related to the phase constant β of the complex, radial, *leaky* wavenumber $k_\rho = \beta - j\alpha$ (being α the attenuation constant [8]) through the relation $\beta = k_0 \sin \theta_0$, with k_0 the free-space wavenumber. (We note that the axicon angle plays in the near field the same role of the beam angle in far field [11].) This simple relation allows for a relatively straightforward design procedure, as is shown next.

A BB is created from the constructive interference between *two cylindrical leaky waves* propagating in the cavity: an *outward* one excited from the central feeder, and an *inward* one due to the reflection of the outward wave onto the metallic rim. In particular, in order to enforce this interference, the metallic rim has to be placed in one of the zeros of the desired Bessel-like distribution. Therefore, a different boundary condition has to be applied depending on whether we deal with TM- or TE-polarized BBs.

For a TM-polarized BB with azimuthal symmetry, the only non-zero components are E_z, E_ρ, and H_ϕ, whereas in the dual, TE-polarized case, they are H_z, H_ρ, E_ϕ. In both cases, the radial profile of the vertical component is proportional to a zeroth order Bessel function, viz., $J_0(k_\rho \rho)$, whereas the radial and azimuthal components are proportional to a first-order Bessel function, viz., $J_1(k_\rho \rho)$ [7], [10].

Consequently, the aperture radius should be set according to the following equation:

$$\beta \rho_{\mathrm{ap}} = j_{nq}, \qquad (2)$$

where j_{nq} is the q-th zero of the n-th order Bessel function, with $n = 0$ in the TM case (as shown in, e.g., [7] and [8]) and $n = 1$ in the TE case (as shown in, e.g., [10]).

In order to obtain a consistent comparison with [6], we considered the same working frequency $f_0 = 30$ GHz and aperture radius $\rho_{\mathrm{ap}} = 15\,\mathrm{mm}$, and enforced the resonance with the second zero $q = 2$. Using these parameters in (2) we have, in the TM case ($n = 0$), $\hat{\beta} = \beta / k_0 \simeq 0.5857$ [6], and, in the TE case ($n = 1$), $\hat{\beta} \simeq 0.7436$. As a result, the nondiffracting range in the TE case is lowered (viz., $z_{\mathbf{ndr}} \simeq 13.5\,\mathrm{mm}$) with respect to that in [6] (viz., $z_{\mathbf{ndr}} \simeq 20\,\mathrm{mm}$).

As shown in [7], once the ρ_{ap}, f_0, and β are fixed, it is important to set the normalized attenuation constant $\hat{\alpha} = \alpha / k_0$ such that $\alpha \rho_{\mathrm{ap}} \ll 1$. This condition ensures that both the outward and the inward cylindrical leaky waves have almost the same amplitude (as required to generate a stationary-like cylindrical aperture field). In principle, one would set $\hat{\alpha}$ as low as possible. However, this may lead to challenges in the PRS design [12], thus we set here $\hat{\alpha} \simeq 0.0027$ as in [6].

The cavity height h and the equivalent PRS reactance X_s required to have these values of $\hat{\beta}$ and $\hat{\alpha}$ are found using a leaky-wave analysis based on an equivalent loss-tangent model [13] and are equal to $h = 7.194$ mm and $X_s = 67.235\,\Omega$, respectively. As typical for this class of structures [5]–[8], the PRS is fully described with a single scalar purely imaginary surface impedance boundary condition $Z_s = jX_s$ (an assumption that is fairly accurate for homogenized PRS such as those analyzed in [12] and references therein).

The accuracy of these approximations can be inferred from Fig. 3, where the dispersion curve of the normalized TE leaky wavenumber is reported along with the radial resonances given by (2) for $n = 1$, and $q = 1, 2, 3$. The intersection between the $q = 2$ radial resonance and $\hat{\beta}$ of the leaky mode yields the working point which is found around $f_0 = 30\,\mathrm{GHz}$, as expected. The dispersion curves of $\hat{\beta}$ and $\hat{\alpha}$ are numerically obtained by solving for the complex *improper* roots of the relevant dispersion equation (see, e.g., [8] for further details).

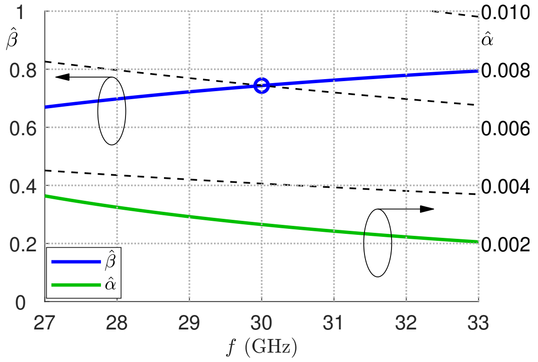

Fig. 3. Dispersion curves of the normalized phase (in blue) and attenuation (in green) constant of the TE leaky mode vs. frequency. The black dashed lines represent the $q = 1$, 2, 3 radial resonances given by (2) for TE modes ($n = 1$) with $\rho_{\mathrm{ap}} = 15$ mm. A blue circle highlights the working point.

With these design parameters at hand, we now need to effectively excite a TE leaky-wave within the cavity. In [9] and [10] loop antennas and coils were used, which are equivalent to VMDs. However, their azimuthal symmetry is necessarily broken by the feeding point and this deteriorates the polarization purity of the excited field. Here instead we approximate a continuous ring of radially directed surface magnetic current through a circular discrete array of radial slots. The former continuous source couples with irrotational transverse magnetic fields only and hence excites a purely TE field; the latter discrete counterparts is still capable of achieving a high polarization purity, provided the number of slots is sufficiently high. Here, we have considered a radial-slot array (see Fig. 2) with $N = 8$ slots of width $w_s = 1$ mm and length $l_s = 2$ mm, uniformly displaced on the ground plane at a radial distance $R = 2.5$ mm from the central axis.

The full-wave simulation of the entire structure and additional numerical validations (not reported for brevity) confirm the effectiveness of this excitation scheme. As is manifest from Fig. 4(a), the near-field distribution obtained with full-wave simulations remarkably agrees with the expected theoretical results. Indeed, the radial dependence of the tangential components of the field (i.e., $\mathbf{E_t}$ and $\mathbf{H_t}$) and of H_z are described by the functions $J_1(\cdot)$ and $J_0(\cdot)$, respectively. It is worthwhile to stress that, in the proposed launcher, the E_z component is 30 dB lower than $||\mathbf{E_t}||$, whereas, in the *hybrid-TE* polarized BB launcher shown in Fig. 4(b), the E_z component is only 10 dB lower than $||\mathbf{E_t}||$.

III. LINK BUDGET ANALYSIS IN A RADIATIVE NEAR-FIELD WIRELESS LINK

The TE-polarized BB launcher described in the previous Section II can fruitfully be exploited to generate a radiative near-field wireless link based on TE-polarized BBs. As shown in [4]–[6], limited-diffractive WPT links can be achieved using two identical launchers one in front of the other. In particular, we consider here two launchers designed according to the description given in Section II.

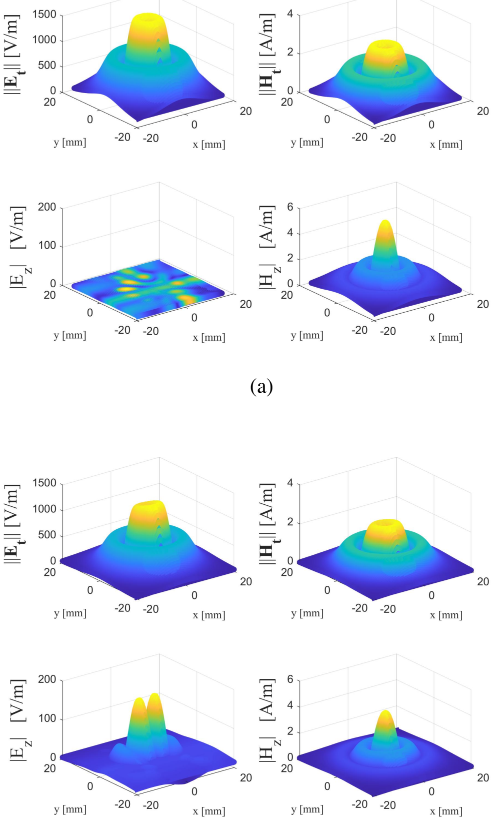

(a)

(b)

Fig. 4. Full-wave results for the (a) TE-polarized BB launcher, and the (b) Hybrid-TE polarized BB launcher [6]. Both field distributions are reported on a xy-plane at $z = 10\,$mm.

In order to perform a safe power budget calculation of this WPT scenario, the general-purpose link budget model described in [14] is exploited and applied considering the designed TE-polarized BB launchers as transmitting (TX) and receiving (RX) antennas. In order to conduct this calculation, we make use of the Norton equivalent circuit of a rectenna [14], whose received power is calculated as:

$$P_{\mathrm{r}} = (1/8)|I_{\mathrm{eq}}|^2/\mathrm{Re}\,[Y_{\mathrm{a}}(\omega)] \tag{3}$$

where $Y_{\mathrm{a}}(\omega)$ is the internal complex admittance of the antenna, i.e., the TE-polarized BB launcher. As can be noticed from (3), performing an accurate computation of the current I_{eq} is key for a correct estimation of the overall power budget.

The current I_{eq} is rigorously calculated applying the power budget algorithm [14] for which the electromagnetic field components of the TX and RX launchers are replaced by the electric and magnetic equivalent surface currents evaluated on a plane interposed between the two launchers. To better compare the performance the integrand of the I_{eq} equation [14] is considered:

$$\hat{\mathbf{n}} \cdot [\mathbf{E}_{\mathrm{i}}(P_{\mathrm{S}}) \times \mathbf{H}_{\mathrm{R}}(P_{\mathrm{S}}) - \mathbf{E}_{\mathrm{R}}(P_{\mathrm{S}}) \times \mathbf{H}_{\mathrm{i}}(P_{\mathrm{S}})] \tag{4}$$

where P_{S} are the points belonging to the interposed surface S, whose normal unit vector is $\hat{\mathbf{n}}$, whereas $\mathbf{E}_{\mathrm{i}}$, $\mathbf{H}_{\mathrm{i}}$, $\mathbf{E}_{\mathrm{R}}$ and

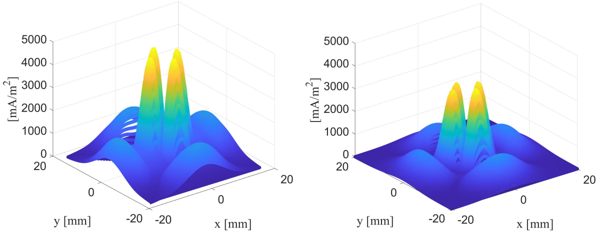

(a) (b)

Fig. 5. Computed equivalent current density for the (a) TE-polarized BB launcher, and the (b) Hybrid-TE polarized BB launcher [6]. Both plots are evaluated on a xy-plane at $z = 10\,\mathrm{mm}$.

Table 1. Received power at 30 GHz for BB launchers with different feeders and polarizations.

TX-RX distance (mm)	P_{r} (dBm) TM [6]	P_{r} (dBm) Hybrid-TE [6]	P_{r} (dBm) **TE (this work)**
20	10.7	6.4	**9.8**
30	5.7	-0.6	**3.2**
40	-0.7	-5.4	**-1.1**

$\mathbf{H}_{\mathrm{R}}$ are the electric and magnetic fields of the TX and RX launchers respectively.

The fields $\mathbf{E}_{\mathrm{i}}$ and $\mathbf{H}_{\mathrm{i}}$ are extracted by the full-wave simulations of a single launcher, the TX, whereas $\mathbf{E}_{\mathrm{R}}$ and $\mathbf{H}_{\mathrm{R}}$, related to the RX, are numerically evaluated allowing for drastically reducing the overall computational time of a full-wave simulation of the entire WPT link. Figure 5(a) shows the computed equivalent current density for the presented TE-polarized BB, whereas Fig. 5(b) refers to the equivalent current density evaluated for the hybrid-TE launcher [6]. Both cases are computed and plotted for a reference distance of $z = 10$ mm. As can be noticed, they both present four main lobes in which the overall equivalent current density is mainly concentrated. However, the TE-polarized case exhibits higher peaks that mirror in a higher receiver power, as is further addressed in the following results.

The received power for different operating distances (namely 20, 30, and 40 mm) is then evaluated and compared. Table 1 shows the received power levels for the considered distances when the input power of the TX launcher is 21 dBm.

As can be inferred from Table 1, the performance of the proposed TE-polarized BB launcher is comparable with respect to that of the TM-polarized one presented in [5], while it exhibits higher received power level with respect to the hybrid-TE version [6]. For this reason, the excitation scheme presented in this work can lead to further valuable realizations of BB launchers to be applied for WPT purposes.

IV. CONCLUSION

This work presents an original efficient excitation scheme for generating TE-polarized BBs in leaky-wave resonant cavities. Specifically, an array of radial slots is etched on the ground plane of a leaky-wave resonant cavity designed to produce a dominant zeroth-order BB over the vertical magnetic field component H_z and a negligible vertical electric field E_z. Full-wave simulations demonstrated that the E_z is indeed negligible, whereas H_z exhibits the desired, focused field profile. The link power budget is finally evaluated showing promising results with respect to the state-of-the-art, paving the way for effective approaches to excite *pure* TE-polarized BBs in WPT scenarios.

ACKNOWLEDGMENT

This work was funded by the Italian Ministry of Education, University and Research (MIUR) within the framework of the PRIN 2017-WPT4WID (‘Wireless Power Transfer for Wearable and Implantable Devices’) ongoing project.

REFERENCES

[1] H. E. Hernández-Figueroa, M. Zamboni-Rached, and E. Recami, *Nondiffracting Waves*. Weinheim, Germany: John Wiley & Sons, 2013.

[2] D. McGloin and K. Dholakia, “Bessel beams: diffraction in a new light,” *Contemporary Phys.*, vol. 46, no. 1, pp. 15–28, 2005.

[3] M. Ettorre, S. C. Pavone, M. Casaletti, M. Albani, A. Mazzinghi, and A. Freni, “Near-field focusing by non-diffracting Bessel beams,” in *Aperture Antennas for Millimeter and Sub-Millimeter Wave Applications*. Cham, Switzerland: Springer, 2018, pp. 243–288.

[4] J. D. Heebl, M. Ettorre, and A. Grbic, “Wireless links in the radiative near field via Bessel beams,” *Phys. Rev. Appl.*, vol. 6, no. 3, p. 034018, Sep. 2016.

[5] F. Benassi, W. Fuscaldo, D. Masotti, A. Galli, and A. Costanzo, “Wireless power transfer in the radiative near-field through resonant Bessel-beam launchers at millimeter waves,” in *2021 IEEE Wireless Power Transf. Conf. (WPTC)*, San Diego, CA, USA, 2021, pp. 1–4.

[6] F. Benassi, W. Fuscaldo, E. Negri, G. Paolini, E. Augello, D. Masotti, P. Burghignoli, A. Galli, and A. Costanzo, “Comparison between hybrid- and TM-polarized Bessel-beam launchers for wireless power transfer in the radiative near-field at millimeter waves,” in *51st Europ. Microw. Conf. (EuMC 2021)*, London, UK, 2022, pp. 1–4.

[7] M. Ettorre, S. M. Rudolph, and A. Grbic, “Generation of propagating Bessel beams using leaky-wave modes: experimental validation,” *IEEE Trans. Antennas Propag.*, vol. 60, no. 6, pp. 2645–2653, Jun. 2012.

[8] W. Fuscaldo, G. Valerio, A. Galli, R. Sauleau, A. Grbic, and M. Ettorre, “Higher-order leaky-mode Bessel-beam launcher,” *IEEE Trans. Antennas Propag.*, vol. 64, no. 3, pp. 904–913, Mar. 2016.

[9] P. Lu, A. Bréard, J. Huillery, X.-S. Yang, and D. Voyer, “Feeding coils design for TE-polarized Bessel antenna to generate rotationally symmetric magnetic field distribution,” *IEEE Antennas Wireless Propag. Lett.*, vol. 17, no. 12, pp. 2424–2428, Dec. 2018.

[10] P. Lu, D. Voyer, A. Bréard, J. Huillery, B. Allard, X. Lin-Shi, and X.-S. Yang, “Design of TE-polarized Bessel antenna in microwave range using leaky-wave modes,” *IEEE Trans. Antennas Propag.*, vol. 66, no. 1, pp. 32–41, Jan. 2017.

[11] D. R. Jackson, P. Burghignoli, G. Lovat, F. Capolino, J. Chen, D. R. Wilton, and A. A. Oliner, “The fundamental physics of directive beaming at microwave and optical frequencies and the role of leaky waves,” *Proc. IEEE*, vol. 99, no. 10, pp. 1780–1805, Oct. 2011.

[12] W. Fuscaldo, S. Tofani, D. C. Zografopoulos, P. Baccarelli, P. Burghignoli, R. Beccherelli, and A. Galli, “Systematic design of THz leaky-wave antennas based on homogenized metasurfaces,” *IEEE Trans. Antennas Propag.*, vol. 66, no. 3, pp. 1169–1178, Mar. 2018.

[13] W. Fuscaldo, “Rigorous evaluation of losses in uniform leaky-wave antennas,” *IEEE Transactions on Antennas and Propagation*, vol. 68, no. 2, pp. 643–655, 2019.

[14] V. Rizzoli, D. Masotti, N. Arbizzani, and A. Costanzo, “CAD procedure for predicting the energy received by wireless scavenging systems in the near- and far-field regions,” in *2010 IEEE MTT-S Int. Microw. Symp.*, 2010, pp. 1768–1771.